CSIAM Trans. Appl. Math.
doi: 10.4208/csiam-am.SO-2021-0051

Vol. **4**, No. 2, pp. 256-274
June 2023

Order Two Superconvergence of the CDG Finite Elements on Triangular and Tetrahedral Meshes

Xiu Ye[1] and Shangyou Zhang[2,*]

[1] *Department of Mathematics, University of Arkansas at Little Rock, Little Rock, AR 72204, USA.*
[2] *Department of Mathematical Sciences, University of Delaware, Newark, DE 19716, USA.*

Received 1 December 2021; Accepted 18 April 2022

Abstract. It is known that discontinuous finite element methods use more unknown variables but have the same convergence rate comparing to their continuous counterpart. In this paper, a novel conforming discontinuous Galerkin (CDG) finite element method is introduced for Poisson equation using discontinuous P_k elements on triangular and tetrahedral meshes. Our new CDG method maximizes the potential of discontinuous P_k element in order to improve the convergence rate. Superconvergence of order two for the CDG finite element solution is proved in an energy norm and in the L^2 norm. A local post-process is defined which lifts a P_k CDG solution to a discontinuous P_{k+2} solution. It is proved that the lifted P_{k+2} solution converges at the optimal order. The numerical tests confirm the theoretic findings. Numerical comparison is provided in 2D and 3D, showing the P_k CDG finite element is as good as the P_{k+2} continuous Galerkin finite element.

AMS subject classifications: 65N15, 65N30

Key words: Finite element, conforming discontinuous Galerkin method, stabilizer free, triangular grid, tetrahedral grid.

1 Introduction

Finite element methods use two different methodologies to approximate the solution of the following second order elliptic problem:

$$-\Delta u = f \quad \text{in } \Omega, \tag{1.1}$$
$$u = g \quad \text{on } \partial\Omega, \tag{1.2}$$

*Corresponding author. *Email addresses:* `xxye@ualr.edu` (X. Ye), `szhang@udel.edu` (S. Zhang)

where Ω is a 2D polygonal domain, or a 3D polyhedral domain. One is the classic conforming finite element method using continuous P_k polynomials for the solution of the PDE (1.1) and another uses discontinuous P_k polynomials. Interior penalty discontinuous Galerkin (IPDG) method in [3] and CDG methods in [28] are the later cases. Since discontinuous P_k polynomial introduces many more degrees of freedom, one would expect higher order convergence for the discontinuous finite element methods. But the current IPDG and CDG methods, using discontinuous P_k elements, have their convergence rates the same as their continuous counterpart, i.e. $\mathcal{O}(h^k)$ in the energy norm and $\mathcal{O}(h^{k+1})$ in the L^2 norm.

In this paper, we will introduce a new CDG method that uses discontinuous P_k polynomials to approximate the solution of the problem (1.1)-(1.2) on triangular and tetrahedral meshes. The finite element formulations of discontinuous element methods tend to be more complex to ensure weak continuity of discontinuous solutions. Sometimes penalty parameter is needed and to be tuned. However our new CDG method has the following simple formulation without stabilizers and penalty parameters: Find $u_h \in V_h$

$$(\nabla_w u_h, \nabla_w v) = (f,v), \quad \forall v \in V_h, \tag{1.3}$$

where ∇_w is the so called weak gradient. In addition, this new CDG method fully utilizes the degrees of freedom of discontinuous P_k polynomial to obtain order two superconvergence of $\mathcal{O}(h^{k+2})$ in an energy norm and $\mathcal{O}(h^{k+3})$ in the L^2 norm. We attribute these good features to the definition of weak derivatives which are specially designed for discontinuous P_k elements. Order two superconvergence of the CDG solution is confirmed theoretically and numerically. Additionally, we define and prove a local post-process which lifts a C^{-1}-P_k CDG solution to a C^{-1}-P_{k+1} with the optimal order convergence of the latter. We may consider this order two superconvergence from the point of the number of degrees of freedom. On triangular meshes, the numbers of degree of freedom of the space C^{-1}-P_k and the space C^0-P_{k+2} are

$$Ch^{-2}(k+1)(k+2), \quad Ch^{-2}(k+2)^2,$$

respectively. On tetrahedral meshes, they are

$$Ch^{-3}(k+2)(k^2+4k+3), \quad Ch^{-3}(k+2)(k^2+4k+4),$$

respectively. In both cases the dimension of the P_k discontinuous polynomial space is slightly less than that of the P_{k+2} continuous polynomial space. But we show both theoretically and numerically that the CDG P_k solution converges as well as the continuous Galerkin P_{k+2} solution.

The weak derivative used in CDG methods was first introduced in the weak Galerkin (WG) finite element method [24]. Then WG methods have been applied for solving various PDEs such as Sobolev equation, the Navier-Stokes equations, the Oseen equations, time-dependent Maxwell's equations, elliptic interface problems, biharmonic equations, etc, [4–6, 8–27, 31, 32]. The CDG method is derived from the WG method by eliminating the degree of freedoms defined on element boundary. The CDG finite element method, introduced in [28], has been studied for diffusion problem [7, 29], and for biharmonic equations [30].

2 Preliminary

Let $\mathcal{T}_h$ be a conforming and quasi-uniform partition of the domain Ω consisting of triangles in 2D, or tetrahedra in 3D. That is, $(\overline{T}_1\cap\overline{T}_2)^0=\emptyset$ or E, a common edge/face-triangle of elements T_1 and T_2. For every element $T\in\mathcal{T}_h$, we denote by h_T its diameter and by $h=\max_{T\in\mathcal{T}_h}h_T$ for $\mathcal{T}_h$. The elements in a quasi-uniform $\mathcal{T}_h$ are uniformly regular, i.e. $h_T\le\gamma_0\rho_T$ for some $\gamma_0>0$, where ρ_T is the diameter of the maximal inscribed ball of T. Denote by $\mathcal{E}_h$ the set of all edges or face-triangles in $\mathcal{T}_h$, and by $\mathcal{E}_h^0=\mathcal{E}_h\backslash\partial\Omega$ the set of all interior edges or triangles.

For the purpose of error analysis, we define a WG (weak Galerkin) finite element space as follows, for $k\ge1$:

$$\tilde{V}_h=\big\{v=\{v_0,v_b\}: v_0|_T\in P_k(T), v_b|_e\in P_{k+1}(e), e\subset\partial T, T\in\mathcal{T}_h, v_b|_{\partial\Omega}=0\big\}. \tag{2.1}$$

Please note that any function $v\in\tilde{V}_h$ has a single value v_b on each edge $e\in\mathcal{E}_h$.

In general, Π_k denotes a generic local L^2 projection onto $\{P_k(T)\}$ or $\{P_k(e)\}$, where $T\in\mathcal{T}_h$ or $e\in\mathcal{E}_h$. $\Pi_k(D)$ denotes the L^2 projection onto $P_k(D)$, where D is one domain. For other local L^2 projections, we include the set that $\Pi_k(\{S_i\})$ is the local L^2 projection onto a product space $\prod_i P_k(S_i)$. In other words, Π_k denotes either $\Pi_k(\mathcal{T}_h)$ or $\Pi_k(\mathcal{E}_h)$. We also combine these two projections as Q_h for $u\in H^1(\Omega)$

$$Q_hu=\{\Pi_ku,\Pi_{k+1}u\}\in\tilde{V}_h. \tag{2.2}$$

For $v=\{v_0,v_b\}\in\tilde{V}_h$, a weak gradient $\nabla_w v$ is a piecewise vector valued polynomial such that on each $T\in\mathcal{T}_h$, $\nabla_w v|_T\in[P_{k+1}(T)]^d$ satisfies

$$(\nabla_w v,\mathbf{q})_T=(\nabla v_0,\mathbf{q})_T+\langle v_b-v_0,\mathbf{q}\cdot\mathbf{n}\rangle_{\partial T},\quad \forall\mathbf{q}\in[P_{k+1}(T)]^d. \tag{2.3}$$

The following lemma is proved in [2].

Lemma 2.1. *For $v=\{v_0,v_b\}\in\tilde{V}_h$, we have*

$$C_1\|v\|_{1,h}\le\|\nabla_w v\|_0\le C_2\|v\|_{1,h}, \tag{2.4}$$

where

$$\|v\|_{1,h}^2=\sum_{T\in\mathcal{T}_h}\Big(\|\nabla v_0\|_{0,T}^2+h_T^{-1}\|v_0-v_b\|_{\partial T}^2\Big).$$

3 CDG finite element scheme

For a given integer $k\geq 1$, let V_h be the CDG finite element space associated with $\mathcal{T}_h$ by

$$V_h=\left\{v\in L^2(\Omega): v|_T\in P_k(T), T\in\mathcal{T}_h\right\}. \tag{3.1}$$

To connect the vector spaces V_h and $\tilde{V}_h$, we define an embedding operator $E_h: V_h\to\tilde{V}_h$ such that for $v\in V_h$

$$E_h v=\{v,v_b\}\in\tilde{V}_h, \tag{3.2}$$

where v_b is an edge-function of v in $\tilde{V}_h$. The art of the CDG method is how to define v_b. For our new CDG method, we choose v_b in such a sophisticated way,

$$v_b|_e=\begin{cases}0, & \text{if} \quad e\subset\partial\Omega,\\ \Pi_{k+1}(E_{k+2,e}v), & \text{if} \quad e\in\mathcal{E}_h^0,\end{cases} \tag{3.3}$$

where $E_{k+2,e}$ is a lifting operator defined next in (3.9). We drop the index e sometimes from $E_{k+2,e}v$, $E_{k+2}v$, when there is no confusion.

Let $e\in\mathcal{E}_h^0$. Let U_e be the union of a patch of n_e triangles (a closed polygon) close to e such that 4 triangles contain the following 4 aligned squares, as illustrated in Fig. 1,

$$\begin{aligned} &S_1=[x_-,x_-+a]\times[y_-,y_-+a], \quad S_2=[x_+,x_++a]\times[y_-,y_-+a],\\ &S_3=[x_+,x_++a]\times[y_+,y_++a], \quad S_4=[x_-,x_-+a]\times[y_+,y_++a],\end{aligned} \tag{3.4}$$

where

$$x_+-x_-=y_+-y_-=\gamma_0^{-1}h, \quad a=\gamma_0 h \tag{3.5}$$

for some constant $\gamma_0>0$. These four squares may rotate or shift together. In 3D, U_e is the union a patch of tetrahedra close to e (a closed polyhedron) such that 8 tetrahedra contain 8 aligned cubes as illustrated in Fig. 1

$$U_e=\cup_{i=1}^{n_e}\overline{T_i}, \tag{3.6}$$

where $\overline{T_i}$ is the closure of T_i.

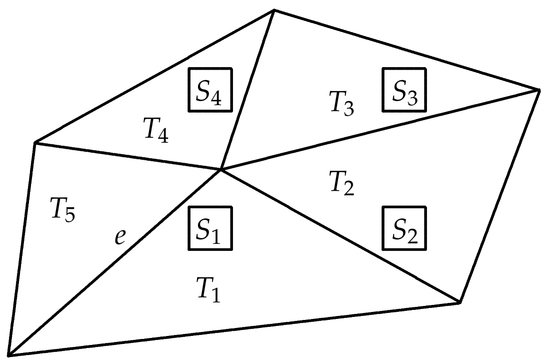

Figure 1: A closed polygon $U_e=\cup_{i=1}^{n_e}\overline{T_i}$ contains 4 aligned squares, for an edge e, where $n_e=5$ and $\overline{T_i}$ is the closure of T_i.

Let $R_e \subset \prod_{i=1}^4 P_k(T_i)$ be the image space of the L^2-projection $\Pi_k(\{S_i\}) : P_{k+2}(U_e) \to \prod_{i=1}^4 P_k(T_i)$,

$$R_e = \{(u_1,\ldots,u_4) \mid u_i = \Pi_k(S_i)u \ \text{ for some } \ u \in P_{k+2}(U_e)\}. \tag{3.7}$$

With R_e we define another L^2 projection $\Pi_e : V_h \cup H^1(\Omega) \to R_e$,

$$(\Pi_e u, v)_{\cup_{i=1}^4 S_i} = (u,v)_{\cup_{i=1}^4 S_i}, \quad \forall v \in R_e. \tag{3.8}$$

We will prove in Lemma 4.1 that when restricted to the subspace R_e the mapping $\Pi_e : P_{k+2}(U_e) \to R_e$ is isomorphic. $\Pi_e^{-1} : R_e \to P_{k+2}(U_e)$ is the inverse mapping. We define

$$E_{k+2,e} = \Pi_e^{-1}\Pi_e : V_h \to P_{k+2}(U_e). \tag{3.9}$$

A function v in V_h does not have its v_b. We let its $v_b = \Pi_{k+1}(E_{k+2,e}v)$. Thus the V_h space is embedded in to $\tilde{V}_h$. Since $E_h v \in \tilde{V}_h$, $\nabla_w E_h v$ can be calculated by (2.3), i.e., for $v \in V_h$, its weak gradient $\nabla_w v$ is defined as

$$\nabla_w v = \nabla_w E_h v. \tag{3.10}$$

The CDG finite element method is to find $u_h \in V_h$ such that

$$(\nabla_w u_h, \nabla_w v) = (f,v), \quad \forall v \in V_h, \tag{3.11}$$

where in the definition of $\nabla_w u_h$, instead of (3.3), $E_h u_h = \{u_h, u_b\} \in \tilde{V}_h$ with

$$u_b|_e = \begin{cases} \Pi_{k+1} g, & \text{if} \quad e \subset \partial\Omega, \\ \Pi_{k+1}(E_{k+2,e}u_h), & \text{if} \quad e \in \mathcal{E}_h^0. \end{cases}$$

Lemma 3.1. *The CDG finite element method* (3.11) *has a unique solution.*

Proof. Let $\varepsilon_h = u_h^1 - u_h^2$, where both u_h^1 and u_h^2 are the CDG solutions of (3.11). Then we have

$$(\nabla_w \varepsilon_h, \nabla_w v) = 0, \quad \forall v \in V_h. \tag{3.12}$$

Letting $v = \varepsilon_h$ in (3.12) gives

$$\|\nabla_w \varepsilon_h\|_0 = 0.$$

Using the equation above, (2.4) and (3.10), we have

$$\|E_h \varepsilon_h\|_{1,h} \le C\|\nabla_w E_h \varepsilon_h\|_0 = C\|\nabla_w \varepsilon_h\|_0 = 0. \tag{3.13}$$

By the definition of $\|\cdot\|_{1,h}$, we have $\nabla \varepsilon_h = 0$ on $T \in \mathcal{T}_h$ and $\varepsilon_h - \varepsilon_b = 0$ on $e \in \mathcal{E}_h$, which imply ε_h is a constant over Ω. By (3.3), we have $\varepsilon_b = 0$ on $\partial\Omega$. Thus $\varepsilon_h = 0$. We complete the proof of the lemma. $\square$

4 Approximation property of the operator $E_{k+2,e}$

Lemma 4.1. *The operator*

$$\Pi_e : P_{k+2}(U_e) \to R_e,$$

defined in (3.8) *is isomorphic if* $k \geq 1$.

Proof. Let the 4 squares $\{S_i\}$ inside some triangles of U_e be defined in (3.4), cf. Fig. 1. We show next the local L^2 projection $\Pi_k(\{S_i\})$ is an injection mapping when restricted on $P_{k+2}(U_e)$

$$\begin{aligned} &\Pi_k : P_{k+2}(U_e) \to R_e, \\ &(\Pi_k u, v)_{S_i} = (u,v)_{S_i}, \quad \forall v \in P_k(T_i), \quad i=1,\dots,4. \end{aligned} \tag{4.1}$$

That is, if $\Pi_k p_{k+2} = 0$ for some $p_{k+2} \in P_{k+2}(U_e)$, then $p_{k+2} = 0$. We expand this $P_{k+2}(U_e)$ polynomial under the product Legendre basis, with the Legendre polynomials $L_i(x)$ obtained by the Gram-Schmidt process under inner product $(\cdot,\cdot)_{(x_-,x_-+a)\cup(x_+,x_++a)}$,

$$p_{k+2}(x,y) = \sum_{0 \leq i+j \leq k+2} c_{ij} L_i(x) L_j(y), \tag{4.2}$$

where

$$\big(L_i(x)L_j(y), L_k(x)L_l(y)\big)_{\cup_{i=1}^4 S_i} = \begin{cases} 1, & \text{if} \quad i=k, \quad j=l, \\ 0, & \text{rest cases.} \end{cases}$$

We will show that all the coefficients of p_{k+2} in (4.2), listed below, are zero,

$$\begin{array}{lllll} c_{k+2,0} & & & & \\ c_{k+1,0} & c_{k+1,1} & & & \\ c_{k,0} & c_{k,1} & c_{k,2} & & \\ \vdots & \cdots & & \ddots & \\ c_{0,0} & c_{0,1} & \cdots & c_{0,k+1} & c_{0,k+2}. \end{array} \tag{4.3}$$

We test (4.2) by two-piece polynomials

$$p(x,y) = \begin{cases} p_1(x)L_0(y) & \text{on } S_1, S_4, \\ p_2(x)L_0(y) & \text{on } S_2, S_3, \end{cases}$$

where $p_1(x)$ and $p_2(x)$ are 1D P_k polynomials. We get

$$\begin{aligned} 0 &= \big(p_{k+2}, p(x,y)\big)_{U_{i=1}^4 S_i} \\ &= \left(\sum_{i=0}^{k+2} c_{i,0} L_i(x), p_1(x)\right)_{(x_-,x_-+a)} + \left(\sum_{i=0}^{k+2} c_{i,0} L_i(x), p_2(x)\right)_{(x_+,x_++a)} \\ &= \big(q_{k+2}(x), p_1(x)\big)_{(x_-,x_-+a)} + \big(q_{k+2}(x), p_2(x)\big)_{(x_+,x_++a)}, \end{aligned}$$

where 1D P_{k+2} polynomial

$$q_{k+2}(x)=\sum_{i=0}^{k+2}c_{i,0}L_i(x)$$

is orthogonal to all two-piece P_k polynomials on $(x_-,x_-+a)\cup(x_+,x_++a)$. We show next $q_{k+2}(x)$ has more than k odd-fold roots inside (x_-,x_-+a), and also inside (x_+,x_++a). We say $x=r$ is an odd-fold root of $q_{k+2}(x)$ if the maximal factor has an odd-integer power n,

$$q_{k+2}(x)=(x-r)^n q_{k+2-n},$$

where $q_{k+2-n}(r)\neq 0$. That is, 1D polynomial $q_{k+2}(x)$ has $2k+2$ or more distinct roots. (This is why we need the condition $k\geq 1$ so that $2k+2>k+2$.) We note that $q_{k+2}(x)$ must change its sign across an odd-fold root. If $q_{k+2}(x)$ has $m(\leq k)$ distinct odd-fold roots in (x_-,x_-+a),

$$x_-<r_1<\cdots<r_m<x_-+a,$$

we let

$$p_1(x)=(x-r_1)\dots(x-r_m)q_{k+2}\left(\frac{x_-+a+r_m}{2}\right)\in P_m(x_-,x_-+a).$$

With this construction, we have

$$\begin{aligned}
&p_1(x)q_{k+2}(x)\geq 0, \quad x\in(x_-,x_-+a),\\
&p_1(x)q_{k+2}(x)>0, \quad x=\frac{x_-+a+r_m}{2}.
\end{aligned}$$

Thus

$$\big(q_{k+2}(x),p_1(x)\big)_{(x_-,x_-+a)}>0.$$

The contradiction implies $m>k$. By the same argument with $p_2(x)$, $q_{k+2}(x)$ has also $m>k$ odd-fold roots in $(0,a)$. Thus, $q_{k+2}(x)$ has $2k+2$ or more roots, and $q_{k+2}(x)\equiv 0$. By the definition of q_{k+2}, we find the coefficients in the first column of (4.3) are all zero, $c_{i,0}=0$ for $i=0,\dots,k+2$.

Repeatedly, we test (4.2) by another two-piece polynomial $p(x)L_1(y)$, where $p(x)\in P_{k-1}(x_-,x_-+a)\times P_{k-1}(x_+,x_++a)$,

$$0=\big(q_{k+1}(x),p(x)\big)_{(x_-,x_-+a)\cup(x_+,x_++a)},$$

where

$$q_{k+1}(x)=\sum_{i=0}^{k+1}c_{i,1}L_i(x).$$

As above, we find q_{k+1} has $2k$ or more roots distinct in $(x_-,x_-+a)\cup(x_+,x_++a)$ and consequently $q_{k+1}\equiv 0$ if $k\geq 2$. Thus all the second-column coefficients $c_{i,1}$ of p_{k+2} in (4.2) are also zero. We can repeat the above selection until the third column from right. That is, we proved that if p_{k+2} in (4.2) has the form

$$\tilde{p}_{k+2}(x,y)=\sum_{l=0}^{k-1} p_{k+2-l}(x)L_l(y), \tag{4.4}$$

then $\tilde{p}_{k+2}(x,y)=0$. If $k\ge 3$, the missing terms of (4.4) are included in an expansion in the other direction

$$p_{k+2}(x,y)-\tilde{p}_{k+2}(x,y)=L_2(x)p_k(y)+L_1(x)p_{k+1}(y)+L_0(x)p_{k+2}(y).$$

Repeating the above argument with x and y exchanged, we get

$$p_{k+2}(x,y)-\tilde{p}_{k+2}(x,y)=0.$$

That is, if $k\ge 3$, to force the last three columns of coefficients in (4.2) to zero, we select testing functions for the bottom three rows, $L_0(x)p_k(y)$, $L_1(x)p_{k-1}(y)$, and $L_2(x)p_{k-2}(y)$, where $p_l(y)$ is a two-piece polynomial. For the same reason as above, we obtain zero for all coefficients of last three rows of p_{k+2} in (4.3). Thus, $p_{k+2}=0$ if $k\ge 3$.

When $k=1$, the polynomial p_{k+2} in (4.2), after above testings, has the following expansion:

$$p_{k+2}(x,y)=c_{1,1}L_1(x)L_1(y)+c_{1,2}L_1(x)L_2(y)+c_{2,1}L_2(x)L_1(y). \tag{4.5}$$

We have to use 4-piece testing polynomials instead of 2-piece polynomials. Let

$$0\ne q_0(x)\in P_0(x_-,x_-+a)\times P_0(x_+,x_++a)$$

be a two-piece P_0 polynomial

$$q_0(x)=\begin{cases}-1, & x\in(x_-,x_-+a),\\ 1, & x\in(x_+,x_++a).\end{cases}$$

Then

$$\big(q_0(x),L_i(x)\big)_{(x_-,x_-+a)\cup(x_+,x_++a)}=\begin{cases}0, & i=0,2,\\ c\ne 0, & i=1.\end{cases}$$

Testing (4.5) by $p(x)q_0(y)$ with $p(x)\in P_1(x_-,x_-+a)\times P_1(x_+,x_++a)$, we get

$$\begin{aligned}0&=c\left(\sum_{i=1}^{2}c_{i,1}L_i(x),p(x)\right)_{(x_-,x_-+a)\cup(x_+,x_++a)}\\ &=c\big(q_2(x),p(x)\big)_{(x_-,x_-+a)\cup(x_+,x_++a)}\end{aligned}$$

and consequently $c_{2,1}=c_{1,1}=0$ as in the proof above for the first and the second columns of coefficients. We test (4.5) by $q_0(x)p(y)$, in the other direction. Then $c_{12}=0$. Therefore $p_{k+2}(x)=0$ if $\Pi_k p_{k+2}(x)=0$, for $k=1$.

For the last case $k=2$, the polynomial p_{k+2} in (4.2), after the earlier testings for $k\geq 3$ and $k=1$, has only one possible non-zero term left

$$p_{k+2}(x,y)=c_{2,2}L_2(x)L_2(y). \tag{4.6}$$

Testing (4.6) by $q_{1/2}(x)q_{1/2}(y)$, where

$$q_{\frac{1}{2}}(x)=\begin{cases}-1, & x\in(x_-,x_-+a),\\ 0, & x\in(x_+,x_++a),\end{cases}$$

we get

$$0=(p_{k+2},1)_{S_1}=c^2c_{2,2}.$$

Here

$$c=\int_{-1}^{-1+a}L_2(x)dx>0.$$

It follows that $c_{2,2}=0$. Therefore, $p_{k+2}(x)=0$ if $\Pi_k p_{k+2}(x)=0$, for $k=2$.

In 3D, the proof of injection is similar that for a triangle e,U_e contains the following eight cubes:

$$S_i=(x_\pm,x_\pm+a)\times(y_\pm,y_\pm+a)\times(z_\pm,z_\pm+a).$$

By the definition of R_e which is the range of $\Pi_e V_h$, Π_e is also on to. Thus Π_e is isomorphic. The lemma is proved. $\square$

Lemma 4.2. *For $k\geq 1$, the projection $E_{k+2,e}\Pi_k: P_{k+2}(U_e)\to P_{k+2}(U_e)$ is the identity mapping, where Π_k is the element-wise L^2 projection to V_h, $E_{k+2,e}$ is defined in* (3.9) *and U_e is defined in* (3.6). *That is,*

$$E_{k+2,e}\Pi_k u=u, \quad \textit{if} \quad u\in P_{k+2}(U_e). \tag{4.7}$$

Proof. Let $u\in P_{k+2}(U_e)$. By definitions of R_e (3.7) and Π_e (3.8)

$$\Pi_e u=\Pi_k u.$$

As $\Pi_e u\in R_e$, $\Pi_e\Pi_e u=\Pi_e u$. By Lemma 4.1 and definition of $E_{k+2,e}$ (3.9), it follows:

$$E_{k+2,e}\Pi_k u=\Pi_e^{-1}\Pi_e\Pi_e u=\Pi_e^{-1}\Pi_e u=u.$$

The proof is complete. $\square$

Lemma 4.3. *For $k\geq 1$, the projection $E_{k+2,e}\Pi_k: H^{k+3}(U_e)\to P_{k+2}(U_e)$ is stable,*

$$\|E_{k+2,e}\Pi_k u\|_{0,U_e}\leq C\|u\|_{0,U_e}, \tag{4.8}$$

where Π_k is the element-wise L^2 projection to V_h, $E_{k+2,e}$ is defined in (3.9) *and U_e is defined in* (3.6). *Further, it is of order $k+3$ accuracy that*

$$\|E_{k+2,e}\Pi_k u-u\|_{0,U_e}\leq Ch^{k+3}|u|_{k+3,U_e}. \tag{4.9}$$

Proof. By the Cauchy-Schwartz inequality, for $u\in H^{k+3}(U_e)$,

$$\|\Pi_k u\|_{0,U_e}^2=(u,\Pi_k u)_{U_e}\le\|u\|_{0,U_e}\|\Pi_k u\|_{0,U_e}.$$

That is,

$$\|\Pi_k u\|_{0,U_e}\le\|u\|_{0,U_e}. \tag{4.10}$$

For $u\in V_h$

$$\|\Pi_e u\|_{0,\cup_{i=1}^4 S_i}^2=(u,\Pi_e u)_{0,\cup_{i=1}^4 S_i}\le\|u\|_{0,\cup_{i=1}^4 S_i}\|\Pi_e u\|_{0,\cup_{i=1}^4 S_i}.$$

It implies

$$\|\Pi_e u\|_{0,\cup_{i=1}^4 S_i}\le\|u\|_{0,\cup_{i=1}^4 S_i}\le\|u\|_{0,U_e}. \tag{4.11}$$

For $u\in V_h$, if $u|_{\cup_{i=1}^4 S_i}\in R_e$, there is a unique $\hat{u}\in P_{k+2}(U_e)$ such that $\Pi_k\hat{u}=u$ on S_i, i.e., $E_{k+2,e}u=\hat{u}$. Let $F(\hat{x},\hat{y})$ be the linear transform

$$F(\hat{x},\hat{y})=(x_-+\hat{x}h,y_-+\hat{y}h)=(x,y),$$

which linear transforms the four reference squares

$$\begin{aligned}&\hat{S}_1=[0,\gamma_0]\times[0,\gamma_0], &&\hat{S}_2=[\gamma_0^{-1},\gamma_0^{-1}+\gamma_0]\times[0,\gamma_0],\\ &\hat{S}_3=[\gamma_0^{-1},\gamma_0^{-1}+\gamma_0]\times[\gamma_0^{-1},\gamma_0^{-1}+\gamma_0], &&\hat{S}_4=[0,\gamma_0]\times[\gamma_0^{-1},\gamma_0^{-1}+\gamma_0]\end{aligned}$$

to S_i, $i=1,\ldots,4$, respectively, according to (3.5). Due to the finite dimensional norm equivalence (easy to prove it), on the same domain $\cup_{i=1}^4\hat{s}_i$, under the isomorphic mapping, we have

$$C_1\|\hat{u}\circ F\|_{0,\cup_{i=1}^4\hat{S}_i}\le\|u\circ F\|_{0,\cup_{i=1}^4\hat{S}_i}\le C_1^{-1}\|\hat{u}\circ F\|_{0,\cup_{i=1}^4\hat{S}_i} \tag{4.12}$$

for some $C_1>0$ depending on γ_0 and polynomial degree k only. Again, by the finite dimensional norm equivalence, we have

$$\|\hat{u}\circ F\|_{0,F^{-1}(U_e)}\le C_2\|\hat{u}\circ F\|_{0,\cup_{i=1}^4\hat{S}_i} \tag{4.13}$$

for some $C_2>0$ depending on γ_0 and polynomial degree k only. Combining above four bounds (4.10)-(4.13), we obtain, for $u\in H^{k+3}(U_e)$

$$\begin{aligned}\|E_{k+2,e}\Pi_k u\|_{0,U_e}&=h^2\|\widehat{\Pi_e\Pi_k u}\circ F\|_{0,F^{-1}(U_e)}\le C_2h^2\|\widehat{\Pi_e\Pi_k u}\circ F\|_{0,\cup_{i=1}^4\hat{S}_i}\\ &\le C_1^{-1}C_2h^2\|\Pi_e\Pi_k u\circ F\|_{0,\cup_{i=1}^4\hat{S}_i}=C_1^{-1}C_2\|\Pi_e\Pi_k u\|_{0,\cup_{i=1}^4 S_i}\\ &\le C_1^{-1}C_2\|\Pi_k u\|_{0,\cup_{i=1}^4 S_i}\le C_1^{-1}C_2\|u\|_{0,U_e}.\end{aligned}$$

Let $p_{k+2}=\Pi_{k+2}(U_e)u$ be the L^2 projection of u on one piece domain U_e. By (4.7) and (4.8), it follows that

$$\begin{aligned}\|E_{k+2}\Pi_k u-u\|_{0,U_e}&\le\|E_{k+2}\Pi_k u-p_{k+2}\|_{0,U_e}+\|p_{k+2}-u\|_{0,U_e}\\ &=\|E_{k+2}\Pi_k(u-p_{k+2})\|_{0,U_e}+\|p_{k+2}-u\|_{0,U_e}\\ &\le(C+1)\|p_{k+2}-u\|_{0,U_e}\le Ch^{k+3}|u|_{k+3,U_e}.\end{aligned}$$

The proof is complete. $\square$

5 Superconvergence in energy norm

In this section, we will obtain order two superconvergence for the CDG finite element solution in (3.11). The superconvergence of the corresponding WG method [2] will be used to achieve such a goal. Let $\tilde{u}_h \in \tilde{V}_h$ be the solution of the WG method in [2] such that

$$(\nabla_w \tilde{u}_h, \nabla_w v) = (f, v_0), \quad \forall v = \{v_0, v_b\} \in \tilde{V}_h. \tag{5.1}$$

The superconvergence of the WG finite element solution $\tilde{u}_h$ is derived in [2] described by the following lemma.

Lemma 5.1. *Let $\tilde{u}_h = \{\tilde{u}_0, \tilde{u}_b\} \in \tilde{V}_h$ be the* WG *finite element solution of* (5.1). *Then*

$$h\|\nabla_w (Q_h u - \tilde{u}_h)\|_0 + \|\Pi_k u - \tilde{u}_0\|_0 \le C h^{k+3} |u|_{k+3}. \tag{5.2}$$

For any function $\varphi \in H^1(T)$, the following trace inequality holds true:

$$\|\varphi\|_e^2 \le C\left(h_T^{-1}\|\varphi\|_T^2 + h_T\|\nabla\varphi\|_T^2\right). \tag{5.3}$$

Lemma 5.2. *Let $u \in H^{k+3}(\Omega)$. Then we have*

$$\|\nabla_w (Q_h u - \Pi_k u)\|_0 \le C h^{k+2} |u|_{k+3}. \tag{5.4}$$

Proof. Recall $Q_h u = \{\Pi_k u, \Pi_{k+1} u\}$ and $E_h \Pi_k u = \{\Pi_k u, \Pi_{k+1} E_{k+2} \Pi_k u\}$. Letting

$$q = \nabla_w (Q_h u - \Pi_k u) \cdot \mathbf{n}$$

in (2.3) and using the trace inequality (5.3), inverse inequality and (4.9) yield

$$\begin{aligned}
&\|\nabla_w (Q_h u - \Pi_k u)\|_0^2 = \|\nabla_w (Q_h u - E_h \Pi_k u)\|_0^2 \\
=& \sum_{T\in\mathcal{T}_h} \langle \Pi_{k+1} u - \Pi_{k+1} E_{k+2} \Pi_k u, q\rangle_{\partial T} = \sum_{T\in\mathcal{T}_h} \langle u - E_{k+2}\Pi_k u, q\rangle_{\partial T} \\
\le& \left(\sum_{T\in\mathcal{T}_h} h_T^{-1} \|u - E_{k+2}\Pi_k u\|_{0,\partial T}^2\right)^{\frac{1}{2}} \left(\sum_{T\in\mathcal{T}_h} h_T \|q\|_{0,\partial T}^2\right)^{\frac{1}{2}} \\
\le& C\left(\sum_{T\in\mathcal{T}_h} h_T^{-2}\|u - E_{k+2}\Pi_k u\|_{0,T}^2 + \|\nabla(u - E_{k+2}\Pi_k u)\|_{0,T}^2\right)^{\frac{1}{2}} \|q\|_0 \\
\le& C h^{k+2} |u|_{k+3} \|\nabla_w (Q_h u - \Pi_k u)\|_0.
\end{aligned} \tag{5.5}$$

We complete the proof of the lemma. ☐

Subtracting (3.11) from (5.1) implies

$$\left(\nabla_w (\tilde{u}_h - u_h), \nabla_w v\right) = 0, \quad \forall v \in V_h. \tag{5.6}$$

The following lemma provides the error bound for $\tilde{u}_h - u_h$.

Lemma 5.3. *Let* $u\in H^{k+3}(\Omega)$*. Then we have*

$$\|\nabla_w(\tilde{u}_h-u_h)\|_0\le Ch^{k+2}|u|_{k+3}. \tag{5.7}$$

Proof. By (5.6),

$$\begin{aligned}\|\nabla_w(\tilde{u}_h-u_h)\|_0^2&=\big(\nabla_w(\tilde{u}_h-u_h),\nabla_w(\tilde{u}_h-u_h)\big)\\&=\big(\nabla_w(\tilde{u}_h-u_h),\nabla_w(\tilde{u}_h-\Pi_k u)\big)\\&\le\|\nabla_w(\tilde{u}_h-u_h)\|_0\,\|\nabla_w(\tilde{u}_h-\Pi_k u)\|_0,\end{aligned} \tag{5.8}$$

which implies

$$\|\nabla_w(\tilde{u}_h-u_h)\|_0\le\|\nabla_w(\tilde{u}_h-\Pi_k u)\|_0. \tag{5.9}$$

Applying the estimates (5.2) and (5.4) to (5.9), we obtain

$$\begin{aligned}\|\nabla_w(\tilde{u}_h-u_h)\|_0&\le\|\nabla_w(\tilde{u}_h-\Pi_k u)\|_0\\&\le\|\nabla_w(\tilde{u}_h-Q_h u)\|_0+\|\nabla_w(Q_h u-\Pi_k u)\|_0\\&\le Ch^{k+2}|u|_{k+3}.\end{aligned} \tag{5.10}$$

The proof is complete. □

The order two superconvergence of the CDG solution in an energy norm is obtained in the following theorem.

Theorem 5.1. *Let* $u\in H^{k+3}(\Omega)\cap H_0^1(\Omega)$ *be the exact solution of* (1.1)*. Let* $u_h\in V_h$ *be the CDG solution of* (3.11)*. Then*

$$\|\nabla_w(\Pi_k u-u_h)\|_0\le Ch^{k+2}|u|_{k+3}. \tag{5.11}$$

Proof. By (5.2), (5.7) and (5.4), we have

$$\begin{aligned}&\|\nabla_w(\Pi_k u-u_h)\|_0\\\le&\|\nabla_w(\Pi_k u-Q_h u)\|_0+\|\nabla_w(Q_h u-\tilde{u}_h)\|_0+\|\nabla_w(\tilde{u}_h-u_h)\|_0\\\le& Ch^{k+2}|u|_{k+3},\end{aligned}$$

which finishes the proof of the theorem. □

6 Superconvergence in L2 norm

We consider the corresponding dual problem: Find a $w\in H_0^1(\Omega)$ such that

$$-\Delta w=\tilde{u}_0-u_h\quad\text{in }\ \Omega. \tag{6.1}$$

Recall that $\tilde{u}_h=\{\tilde{u}_0,\tilde{u}_b\}$ and u_h are the solutions of the WG method (5.1) and the CDG method (3.11) respectively. Assume that the following H^2-regularity holds:

$$\|w\|_2\le C\|\tilde{u}_0-u_h\|_0. \tag{6.2}$$

In the next theorem, we will prove the order two superconvergence of the CDG solution in the L^2-norm.

Theorem 6.1. *Let $u\in H^{k+3}(\Omega)\cap H_0^1(\Omega)$ be the exact solution of* (1.1). *Let $u_h\in V_h$ be the CDG solution of* (3.11). *Then*

$$\|\Pi_k u-u_h\|_0\le Ch^{k+3}|u|_{k+3}. \tag{6.3}$$

Proof. Let $\tilde{w}_h\in\tilde{V}_h$ be the solution of WG method defined in (5.1) for the problem (6.1) such that

$$(\nabla_w\tilde{w}_h,\nabla_w v)=(\tilde{u}_0-u_h,v_0),\quad \forall v=\{v_0,v_b\}\in\tilde{V}_h. \tag{6.4}$$

Letting $v=\tilde{u}_h-E_hu_h\in\tilde{V}_h$ in (6.4) and by (5.6) and (3.10), we have

$$\begin{aligned}\|\tilde{u}_0-u_h\|_0^2&=\big(\nabla_w\tilde{w}_h,\nabla_w(\tilde{u}_h-u_h)\big)\\&=\big(\nabla_w(\tilde{w}_h-\Pi_kw),\nabla_w(\tilde{u}_h-u_h)\big)\\&\le\|\nabla_w(\tilde{w}_h-\Pi_kw)\|_0\|\nabla_w(\tilde{u}_h-u_h)\|_0.\end{aligned} \tag{6.5}$$

It follows from the estimates (5.2) and (5.4)

$$\|\nabla_w(\tilde{w}_h-\Pi_kw)\|_0\le\|\nabla_w(\tilde{w}_h-Q_hw)\|_0+\|\nabla_w(Q_hw-\Pi_kw)\|_0\le Ch\|w\|_2. \tag{6.6}$$

Using (6.6) and (5.7), (6.5) becomes,

$$\begin{aligned}\|\tilde{u}_0-u_h\|_0^2&\le\|\nabla_w(\tilde{w}_h-\Pi_kw)\|_0\;\|\nabla_w(\tilde{u}_h-u_h)\|_0\\&\le Ch|w|_2\|\nabla_w(\tilde{u}_h-u_h)\|_0\le Ch^{k+3}|u|_{k+3}\|w\|_2.\end{aligned} \tag{6.7}$$

It follows from (6.7) and (6.2)

$$\|\tilde{u}_0-u_h\|_0\le Ch^{k+3}|u|_{k+3}. \tag{6.8}$$

Using (5.2) and (6.8), we have

$$\|\Pi_ku-u_h\|_0\le\|\Pi_ku-\tilde{u}_0\|_0+\|\tilde{u}_0-u_h\|_0\le Ch^{k+3}|u|_{k+3}.$$

We have proved the theorem. □

7 A locally lifted P_{k+2} solution

As we proved that the P_k conforming discontinuous Galerkin solution is two-order superconvergent in both L^2 norm and H^1-like norm, we can use the superconvergent function and its superconvergent weak gradient to define a local post-process, which lifts such a P_k solution to an optimal-order P_{k+2} solution.

On each element T, we solve a local problem that finds $\hat{u}_h\in\Pi_{T\in\mathcal{T}_h}P_{k+2}(T)$ by

$$(\nabla\hat{u}_h-\nabla_wu_h,\nabla v)_T=0,\quad\forall v\in P_{k+2}(T)\setminus P_0(T), \tag{7.1}$$

$$(\hat{u}_h-u_h,v)_T=0,\qquad\forall v\in P_0(T). \tag{7.2}$$

Letting $u_h=0$ in (7.1), we get that $\|\nabla\hat{u}_h\|_0^2=0$ and $\hat{u}_h$ is a constant on each T. By (7.2), the constant is zero. Thus (7.1)-(7.2) has a unique solution. As the linear system is square and finite dimensional, the uniqueness implies the existence of solution.

Theorem 7.1. *Let $u \in H_0^1(\Omega) \cap H^{k+3}(\Omega)$ be the exact solution of the problem* (1.1)-(1.2). *Let $\hat{u}_h \in \Pi_{T\in\mathcal{T}_h} P_{k+2}(T)$ be the locally lifted solution of* (7.1)-(7.2). *Then there exists a constant C such that*

$$\|u-\hat{u}_h\|_0 \le Ch^{k+3}|u|_{k+3}. \tag{7.3}$$

Proof. (7.2) means that

$$\Pi_0 \hat{u}_h = \Pi_0 u_h.$$

We separate the error into two parts

$$\|u-\hat{u}_h\|_0 \le \|\Pi_0(u-\hat{u}_h)\|_0 + \|(I-\Pi_0)(u-\hat{u}_h)\|_0.$$

For the P_0 error, by (6.3), we have

$$\|\Pi_0(u-\hat{u}_h)\|_0 = \|\Pi_0(\Pi_k u - u_h)\|_0 \le \|\Pi_k u - u_h\|_0 \le Ch^{k+3}|u|_{k+3}.$$

For the P_0-orthogonal error, we separate it further into two

$$\begin{aligned}
\|(I-\Pi_0)(u-\hat{u}_h)\|_0 &\le Ch\|\nabla(u-\hat{u}_h)\|_0 \\
&\le Ch\|\nabla(u-\Pi_{k+2}u)\|_0 + Ch\|\nabla(\Pi_{k+2}u-\hat{u}_h)\|_0 \\
&\le Ch^{k+3}|u|_{k+3} + Ch\|\nabla(\Pi_{k+2}u-\hat{u}_h)\|_0.
\end{aligned}$$

In [1], it is proved that

$$\nabla_w(Q_h u) = \Pi_{k+1}\nabla u. \tag{7.4}$$

By (7.4), (7.1) and (5.11),

$$\begin{aligned}
&\|\nabla(\Pi_{k+2}u-\hat{u}_h)\|_0^2 \\
=& \big(\nabla(\Pi_{k+2}u-u), \nabla(\Pi_{k+2}u-\hat{u}_h)\big) + \big(\nabla u - \Pi_{k+1}\nabla u, \nabla(\Pi_{k+2}u-\hat{u}_h)\big) \\
&+ \big(\nabla_w Q_h u - \nabla_w u_h, \nabla(\Pi_{k+2}u-\hat{u}_h)\big) \\
\le& \big(\|\nabla(\Pi_{k+2}u-u)\|_0 + \|\nabla u - \Pi_{k+1}\nabla u\|_0 + \|\nabla_w(Q_h u - u_h)\|_0\big) \cdot \|\nabla(\Pi_{k+2}u-\hat{u}_h)\|_0 \\
\le& Ch^{k+2}|u|_{k+3}\|\nabla(\Pi_{k+2}u-\hat{u}_h)\|_0.
\end{aligned}$$

Combining above three inequalities, (7.3) is proved. □

8 Numerical experiments

In first example, we solve the 2D elliptic equation (1.1) on the domain $\Omega = (0,1)^2$. The function f is chosen so that the exact solution is

$$u = x^2(1-x)^2 y^2(1-y)^2. \tag{8.1}$$

We use triangular grids shown as in Fig. 2. Here each square is subdivided in to 8 trian-

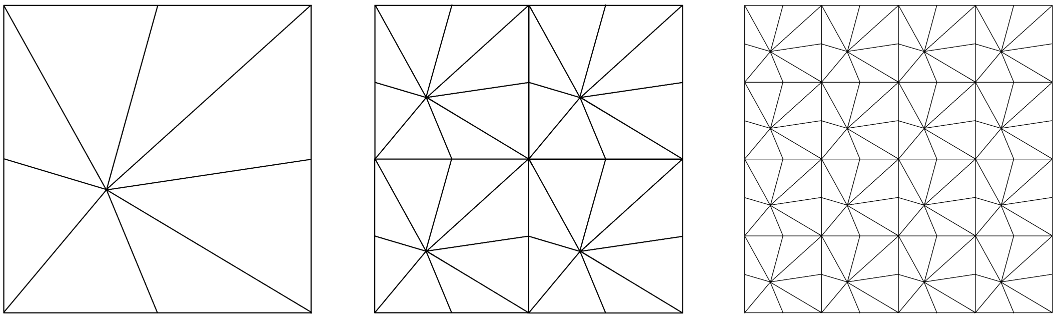

Figure 2: The first three grids for the computation in Tables 1-2.

gles. For all 16 edges on the triangle, U_e is the union of all 8 triangles, i.e., the whole square. We compute this example by four CDG finite elements and four continuous Galerkin finite elements. The results for the four CDG elements are listed in Table 1. For all cases, we get two orders of superconvergence in both L^2 and H^1 norms.

We then lift the P_k CDG finite element solution to a P_{k+2} solution. The results are listed in Table 2. In all cases, the lifted solution converges two-orders higher than that of the original P_k solution. For a comparison, we also list the results for continuous Galerkin P_{k+2} finite element solutions. Also we list the dimension of both finite element spaces. We can see, even though with two-order superconvergence, that the P_k CDG solution is slightly worse than P_{k+2} CG solution.

Table 1: Error profiles and convergence rates for solution (8.1).

Grid	$\|\Pi_k u - u_0\|_0$	Rate	$\|\nabla_w(\Pi_k u - u_h)\|_0$	Rate
	By the P_1 CDG finite element			
5	0.2442E-07	4.1	0.7799E-05	2.9
6	0.1467E-08	4.1	0.1002E-05	3.0
7	0.9017E-10	4.0	0.1270E-06	3.0
	By the P_2 CDG finite element			
4	0.3678E-07	4.8	0.6206E-05	3.7
5	0.1210E-08	4.9	0.4272E-06	3.9
6	0.3859E-10	5.0	0.2803E-07	3.9
	By the P_3 CDG finite element			
3	0.1346E-06	5.2	0.1418E-04	4.4
4	0.2535E-08	5.7	0.5137E-06	4.8
5	0.4302E-10	5.9	0.1714E-07	4.9
	By the P_4 CDG finite element			
4	0.556E-08	6.4	0.821E-06	5.3
5	0.486E-10	6.8	0.145E-07	5.8
6	0.423E-12	6.8	0.234E-09	6.0

Table 2: Error profiles of P_k CDG solutions and P_{k+2} CG solutions for (8.1).

	$\|u-u_h\|_0$	Rate	$\|u-\hat{u}_h\|_0$	Rate	$\dim V_h$	$\dim V_h^c$	$\|u-u_h^c\|_0$	Rate
	By P_1 CDG element and its lift					By P_3 CG element		
5	0.1549E-05	2.0	0.2964E-07	4.1	6144	2401	0.1557E-08	4.0
6	0.3872E-06	2.0	0.1711E-08	4.1	24576	9409	0.9706E-10	4.0
7	0.9682E-07	2.0	0.1084E-09	4.0	98304	37249	0.6057E-11	4.0
	By P_2 CDG element and its lift					By P_4 CG element		
4	0.6425E-06	3.0	0.4324E-07	4.8	3072	4225	0.1175E-08	5.0
5	0.8093E-07	3.0	0.1432E-08	4.9	12288	16641	0.3618E-10	5.0
6	0.1014E-07	3.0	0.4586E-10	5.0	49152	66049	0.1121E-11	5.0
	By P_3 CDG element and its lift					By P_5 CG element		
3	0.6192E-06	3.9	0.1527E-06	5.2	1280	1681	0.3305E-08	6.0
4	0.3964E-07	4.0	0.2846E-08	5.7	5120	6561	0.5140E-10	6.0
5	0.2496E-08	4.0	0.4808E-10	5.9	20480	25921	0.7992E-12	6.0
	By P_4 CDG element and its lift					By P_6 CG element		
2	0.1944E-05	4.8	0.1012E-05	4.7	480	625	0.2059E-07	6.9
3	0.6427E-07	4.9	0.9895E-08	6.7	1920	2401	0.1616E-09	7.0
4	0.2037E-08	5.0	0.8488E-10	6.9	7680	9409	0.1260E-11	7.0

In second example, we solve the 3D elliptic equation (1.1) on the unit cube domain $\Omega=(0,1)^3$. The function f is chosen so that the exact solution is

$$u=\sin(\pi x)\sin(\pi y)\sin(\pi z). \tag{8.2}$$

We use tetrahedral grids shown as in Fig. 3, where each cube is subdivided in to 16 tetrahedra. For all 40 triangles on a cube (both on surface and inside), U_e is the union of all 16 tetrahedra, i.e., the whole cube. We compute this example by three CDG finite elements and three continuous Galerkin finite elements. The results for the four CDG elements are listed in Table 3. For all cases, we get two orders of superconvergence in both L^2 and H^1 norms.

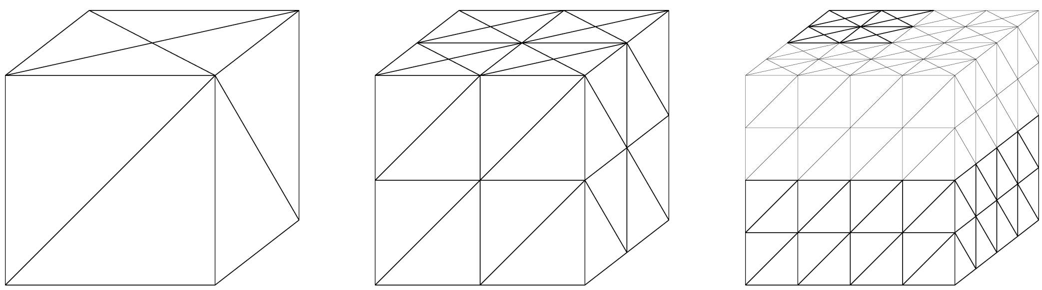

Figure 3: The first three grids for the computation in Tables 1-2.

Table 3: Error profiles and convergence rates for solution (8.2).

Grid	$\|\Pi_k u - u_0\|_0$	Rate	$\|\nabla_w(\Pi_k u - u_h)\|_0$	Rate
	By 3D P_1 CDG element			
4	0.4029E-04	4.18	0.5949E-02	2.96
5	0.2426E-05	4.05	0.7526E-03	2.98
6	0.1503E-06	4.01	0.9468E-04	2.99
	By 3D P_2 CDG element			
3	0.8128E-04	4.97	0.8495E-02	3.69
4	0.2483E-05	5.03	0.5557E-03	3.93
5	0.7664E-07	5.02	0.3519E-04	3.98
	By 3D P_3 CDG element			
2	0.5300E-03	6.40	0.2647E-01	5.04
3	0.9307E-05	5.83	0.1034E-02	4.68
4	0.1433E-06	6.02	0.3437E-04	4.91

Table 4: Error profiles of P_k CDG solutions and P_{k+2} CG solutions for (8.2).

	$\|u - u_h\|_0$	Rate	$\|u - \hat{u}_h\|_0$	Rate
	By 3D P_1 CDG element and its lift			
4	0.1735E-02	2.06	0.1877E-04	3.85
5	0.4312E-03	2.01	0.1229E-05	3.93
6	0.1077E-03	2.00	0.7796E-07	3.98
	By 3D P_2 CDG element and its lift			
3	0.1156E-02	3.05	0.9807E-04	4.90
4	0.1451E-03	2.99	0.3057E-05	5.00
5	0.1820E-04	3.00	0.9510E-07	5.01
	By 3D P_3 CDG element and its lift			
2	0.2106E-02	4.44	0.2913E-03	7.74
3	0.1369E-03	3.94	0.7674E-05	5.25
4	0.8722E-05	3.97	0.1876E-06	5.35

We then lift the 3D P_k CDG finite element solution to a P_{k+2} solution. The results are listed in Table 4. In all cases, the lifted solution converges two orders higher than that of the original P_k solution. For a comparison, in Table 5, we list the results for 3D continuous Galerkin P_{k+2} finite element solutions. Also we list the dimension of both finite element spaces in Table 5. We can see, even with two-order superconvergence, that the P_k CDG solution in 3D is slightly worse than P_{k+2} CG solution. But CDG space dimension is bigger than that of continuous finite element space.

Table 5: Error profiles of P_k CDG solutions and P_{k+2} CG solutions for (8.2).

	$\|u-\hat{u}_h\|_0$	Rate	$\dim V_h$	$\dim V_h^c$	$\|u-u_h^c\|_0$	Rate
	By 3D P_1 CDG's lift			By 3D P_3 CG element		
4	0.1877E-04	3.85	32768	39753	0.7717E-05	4.00
5	0.1229E-05	3.93	262144	308369	0.4814E-06	4.00
6	0.7796E-07	3.98	2097152	2429217	0.3007E-07	4.00
	By 3D P_2 CDG's lift			By 3D P_4 CG element		
3	0.9807E-04	4.90	10240	12081	0.1102E-04	4.84
4	0.3057E-05	5.00	81920	92257	0.3550E-06	4.96
5	0.9510E-07	5.01	655360	721089	0.1118E-07	4.99
	By 3D P_3 CDG's lift			By 3D P_5 CG element		
2	0.2913E-03	7.74	2560	3111	0.4302E-04	3.78
3	0.7674E-05	5.25	20480	23101	0.7032E-06	5.94
4	0.1876E-06	5.35	163840	178041	0.1106E-07	5.99

References

[1] A. Al-Twaeel, S. Hussian, and X. Wang, *A stabilizer free weak Galerkin finite element method for parabolic equation*, J. Comput. Appl. Math., 392:113373, 2021.

[2] A. Al-Taweel, X. Wang, X. Ye, and S. Zhang, *A stabilizer free weak Galerkin method with supercloseness of order two*, Numer. Methods Partial Differ. Equ., 37:1012–1029, 2021.

[3] D. N. Arnold, *An interior penalty finite element method with discontinuous elements*, SIAM J. Numer. Anal., 19(4):742–760, 1982.

[4] G. Chen, M. Feng, and X. Xie, *A robust WG finite element method for convection–diffusion–reaction equations*, J. Comput. Appl. Math., 315:107–125, 2017.

[5] W. Chen, F. Wang, and Y. Wang, *Weak Galerkin method for the coupled Darcy–Stokes flow*, IMA J. Numer. Anal., 36:897–921, 2016.

[6] M. Cui and S. Zhang, *On the uniform convergence of the weak Galerkin finite element method for a singularly-perturbed biharmonic equation*, J. Sci. Comput., 82:5–15, 2020.

[7] Y. Feng, Y. Liu, R. Wang, and S. Zhang, *A conforming discontinuous Galerkin finite element method on rectangular partitions*, Electron. Res. Arch., 29:2375–2389, 2021.

[8] Q. Guan, *Weak Galerkin finite element method for Poisson's equation on polytopal meshes with small edges or faces*, J. Comput. Appl. Math., 368:112584, 2020.

[9] Q. Hu, Y. He, and K. Wang, *Weak Galerkin method for the Helmholtz equation with DTN boundary condition*, Int. J. Numer. Anal. Model., 17:643–661, 2020.

[10] X. Hu, L. Mu, and X. Ye, *A weak Galerkin finite element method for the Navier-Stokes equations on polytopal meshes*, J. Comput. Appl. Math., 362:614–625, 2019.

[11] W. Huang and Y. Wang, *Discrete maximum principle for the weak Galerkin method for anisotropic diffusion problems*, Commun. Comput. Phys., 18:65–90, 2015.

[12] G. Li, Y. Chen, and Y. Huang, *A new weak Galerkin finite element scheme for general second-order elliptic problems*, J. Comput. Appl. Math., 344:701–715, 2018.

[13] H. Li, L. Mu, and X. Ye, *Interior energy estimates for the weak Galerkin finite element method*, Numer. Math., 139:447–478, 2018.

[14] R. Lin, X. Ye, S. Zhang, and P. Zhu, *A weak Galerkin finite element method for singularly perturbed convection-diffusion-reaction problems*, SIAM J. Numer. Anal., 56:1482–1497, 2018.
[15] J. Liu, S. Tavener, and Z. Wang, *Lowest-order weak Galerkin finite element method for Darcy flow on convex polygonal meshes*, SIAM J. Sci. Comput., 40:1229–1252, 2018.
[16] J. Liu, S. Tavener, and Z. Wang, *The lowest-order weak Galerkin finite element method for the Darcy equation on quadrilateral and hybrid meshes*, J. Comput. Phys., 359:317330, 2018.
[17] X. Liu, J. Li, and Z. Chen, *A weak Galerkin finite element method for the Oseen equations*, Adv. Comput. Math., 42:1473–1490, 2016.
[18] L. Mu, X. Ye, and S. Zhang, *A stabilizer free, pressure robust and superconvergence weak Galerkin finite element method for the Stokes equations on polytopal mesh*, SIAM J. Sci. Comput., 43:A2614–A2637, 2021.
[19] N. Noon, *Weak Galerkin and weak group finite element methods for 2-D Burgers problem*, Journal of Advanced Research in Fluid Mechanics and Thermal Sciences, 69(2):42–59, 2020.
[20] S. Shields, J. Li, and E. A. Machorro, *Weak Galerkin methods for time-dependent Maxwell's equations*, Comput. Math. Appl., 74:2106–2124, 2017.
[21] M. Sun and H. Rui, *A coupling of weak Galerkin and mixed finite element methods for poroelasticity*, Comput. Math. Appl., 73:804–823, 2017.
[22] S. Toprakseven, *A weak Galerkin finite element method for time fractional reaction-diffusion-convection problems with variable coefficients*, Appl. Numer. Math., 168:1–12, 2021.
[23] C. Wang and J. Wang, *Discretization of div–curl systems by weak Galerkin finite element methods on polyhedral partitions*, J. Sci. Comput., 68:1144–1171, 2016.
[24] J. Wang and X. Ye, *A weak Galerkin finite element method for second-order elliptic problems*, J. Comput. Appl. Math., 241:103–115, 2013.
[25] J. Wang, Q. Zhai, R. Zhang, and S. Zhang, *A weak Galerkin finite element scheme for the Cahn-Hilliard equation*, Math. Comp., 88:211–235, 2019.
[26] Y. Xie and L. Zhong, *Convergence of adaptive weak Galerkin finite element methods for second order elliptic problems*, J. Sci. Comput., 86, 17, 2021.
[27] X. Ye and S. Zhang, *A stabilizer free weak Galerkin method for the biharmonic equation on polytopal meshes*, SIAM J. Numer. Anal., 58:2572–2588, 2020.
[28] X. Ye and S. Zhang, *A conforming discontinuous Galerkin finite element method*, Int. J. Numer. Anal. Model., 17(1):110–117, 2020.
[29] X. Ye and S. Zhang, *A conforming discontinuous Galerkin finite element method: Part II*, Int. J. Numer. Anal. Model., 17:281–296, 2020.
[30] X. Ye and S. Zhang, *A conforming DG method for the biharmonic equation on polytopal meshes*, arXiv:1907.10661.
[31] J. Zhang, K. Zhang, J. Li, and X. Wang, *A weak Galerkin finite element method for the Navier-Stokes equations*, Commun. Comput. Phys., 23:706–746, 2018.
[32] T. Zhang and T. Lin, *A posteriori error estimate for a modified weak Galerkin method solving elliptic problems*, Numer. Methods Partial Differential Equations, 33:381–398, 2017.